

SIMPLE COMPUTATIONAL METHOD FOR COHESIVE CRACK IN CONCRETE-LIKE MATERIALS

J.M. Sancho¹, J. Planas², D. Cendón², E. Reyes³ and J.C. Gálvez³

¹ Dep. de Estructuras de Edificación, E.T.S. Arquitectura, Universidad Politécnica de Madrid, 28040 Madrid, Spain.

² Dep. Ciencia de Materiales, E.T.S.I Caminos, Universidad Politécnica de Madrid, 28040 Madrid, Spain.

³ E.T.S. Ingenieros de Caminos, Universidad de Castilla La Mancha, 13071 Ciudad Real, Spain.

ABSTRACT

This paper presents a numerical implementation of cohesive crack model for the analysis of concrete damage and fracture based on elements with embedded strong discontinuity. A simple central force model is used for the stress vs. crack opening law. The only material data required are the elastic constants and the mode I softening curve. The need for a tracking algorithm is avoided by using a consistent procedure for the selection of the separated nodes, and by letting the crack embedded in the finite element to adapt itself to the stress field while the crack opening does not exceed a small threshold value. Numerical simulations of well known experiments are presented to show the ability of the proposed model to simulate fracture of concrete.

1 INTRODUCTION

Considerable effort has been applied to develop robust numerical algorithms to describe tensile fracture in concrete and other quasibrittle materials. The elder approaches to the finite element modeling of fracture, the smeared crack and the discrete crack, have been in the past years successfully complemented by the application of the so-called strong discontinuity approach (SDA) [1,2]. In contrast to the smeared crack model, in the SDA the fracture zone is represented as a discontinuous displacement surface. In contrast to the discrete crack approach, in the SDA the crack is not restricted to inter-element lines, as the displacement jumps are embedded in the finite element displacement field. For a comparative study of the various approaches to the embedded crack concept proposed in the literature the reader is addressed to Jirásek [3].

A problem of this approach is that, as the additional modes are determined at the element level, the progress of the crack may lock because of kinematical incompatibility between the cracks in neighboring elements.[3,4]

One solution to avoid this problem is to use an algorithm to reestablish the geometric continuity of the crack line across the elements, a procedure known as crack tracking [5]. Most practical implementations use tracking to avoid crack locking. Moreover, some implementations further require establishing exclusion zones defined to avoid the formation of new cracks in the neighborhood of existing cracks. This kind of algorithms constitute an inconvenient to the implementation of the embedded crack elements in standard finite element programs, because the element local character is lost [6] and is therefore of the greater interest to study formulations that circumvent the need for enforcing crack path continuity [7].

In the SDA the discontinuity can be approximated as the limit case of a weak discontinuity where a bandwidth parameter tends to zero [2,8]. In this way the discrete constitutive model for the discontinuity naturally arises from the continuum model. However, for tensile fracture, it is simpler and more effective to use a cohesive crack model that relates the tractions and the displacement jump (crack opening). This approach is used in the present work, which describes a simple method in which the cracking follows from purely local conditions without any need for tracking.

2 BASIC FORMULATION

Although more abstract and general formulations are possible [9] we stick here to a short description of the actual implementation, based on a simple constant stress triangle with strong discontinuity kinematics and a simple central-force cohesive crack model.

Figure 1a shows the triangle after cracking. The basic geometrical parameters are: the crack normal \mathbf{n} , the solitary node S and the gradient \mathbf{b}^+ of the standard (linear) shape function associated to the solitary node. In the standard formulation, the geometry parameters remain fixed once the crack is formed. The only kinematical variable of the crack is the crack opening vector \mathbf{w} (the displacement jump).

We assume that the material outside the crack remains linear elastic, and then the standard analysis of the continuum strain shows that the stress can be written as

$$\boldsymbol{\sigma} = \mathbf{E}:\boldsymbol{\varepsilon}^a - \mathbf{E}:(\mathbf{b}^+ \otimes \mathbf{w})^S, \quad (1)$$

where $\boldsymbol{\sigma}$ = stress tensor, \mathbf{E} = fourth-order tensor of elastic moduli, $\boldsymbol{\varepsilon}^a$ = apparent strain tensor, computed from nodal displacements and standard shape functions; the double dot ($:$) indicates double contraction, the symbol \otimes indicates tensor product of two vectors and super index S denotes the symmetric part of a tensor.

The crack opening is obtained from the equilibrium condition of the crack stated locally (i.e. the traction vector \mathbf{t} on the crack face is equal to the continuum traction $\boldsymbol{\sigma} \cdot \mathbf{n}$), by setting that the crack traction is uniquely related to the history of the crack opening vector. In the present work it is assumed that the forces are central, i.e., that \mathbf{t} and \mathbf{w} are proportional as depicted in Fig. 1b, and that the loading behavior is described by a softening curve, and the unloading-reloading is linear through the origin (Fig. 1b). The resulting equation is

$$\frac{f(\varpi)}{\varpi} \mathbf{w} = \mathbf{n} \cdot \mathbf{E}:\boldsymbol{\varepsilon}^a - (\mathbf{n} \cdot \mathbf{E} \cdot \mathbf{b}^+) \cdot \mathbf{w} \quad \text{with} \quad \varpi = \max(|\mathbf{w}|), \quad (2)$$

where ϖ is the mode I equivalent crack opening, and $f(\varpi)$ is the standard mode I softening curve for the cohesive crack, which can, and should, be determined from standard tests (no mode II parameters are required); as before a double dot means double contraction and a dot a single contraction of indices.

With this, the formulation of the element is complete: given the nodal displacements, $\boldsymbol{\varepsilon}^a$ is first computed in the standard way, then eqn (2) is solved for \mathbf{w} by Newton-Raphson method and the stress then follows from eqn (1). The formation of the stiffness matrix of the element is easily handled by linearizing the foregoing equations.

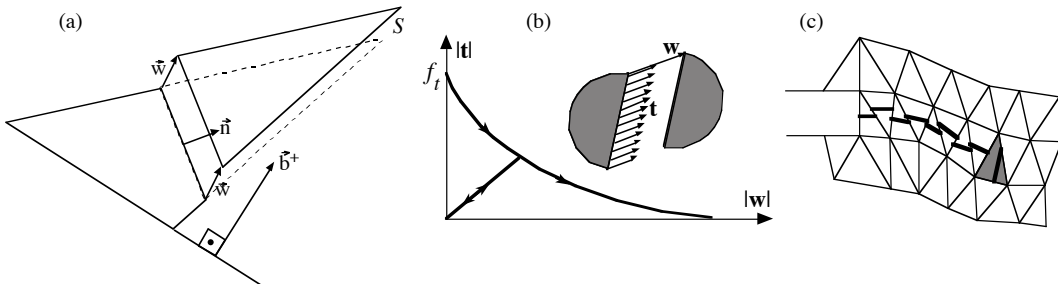


Figure 1: Constant stress triangle(a); softening curve for the cohesive crack model (b); sketch of crack locking (c): bad prediction of cracking direction in the shaded element.

The foregoing equations hold after the crack has been formed. Initially, the behavior is linear elastic, $\mathbf{w} = \mathbf{0}$ in the element, and \mathbf{n} and \mathbf{b}^+ are undefined. Thus, $\boldsymbol{\sigma} = \mathbf{E}:\boldsymbol{\varepsilon}^a$ until the maximum principal stress exceeds the tensile strength. Then a crack is introduced perpendicular to the direction of the maximum principal stress, and \mathbf{n} is computed as the unit eigenvector of $\boldsymbol{\sigma}$ associated to the maximum eigenvalue.

Next, the solitary node and the vector \mathbf{b}^+ are determined by requiring that the angle between \mathbf{n} and \mathbf{b}^+ be the smallest possible (see Fig. 1a). This is equivalent to selecting the solitary node so that the side opposite to it be as parallel as possible to the crack. This procedure was devised based on the observation of Borja [10] that the behavior of this type of element is best when the crack meets such condition, and also based on the analysis in [9] showing that the local and global equilibrium in the element are simultaneously met only when \mathbf{n} is parallel to \mathbf{b}^+ . [Note that the iterative procedure to solve (2) cannot start with $\mathbf{w} = \mathbf{0}$ because of infinite tangential stiffness; thus the first iteration after crack initiation requires a finite initial value; various strategies are possible, but the simplest one is to start iterating with $\mathbf{w}^0 = c \mathbf{n}$ where c is a small value of the order of $0.0001 G_F/f_t$. Here, G_F is the fracture energy and f_t the tensile strength.]

3 CRACK LOCKING AND CRACK ADAPTATION

The foregoing procedure is a variant of the so called SKON approach (statically and kinematically optimal non-symmetric) [3] and is strictly local: no crack continuity is enforced or crack exclusion zone defined. This leads in many circumstances to locking after a certain crack growth, as will be seen in an example later on. Such locking seems to be due to a bad prediction of the cracking direction in the element ahead of the pre-existing crack, as sketched in Figure 1c.

To overcome this problem without introducing global algorithms (crack tracing and exclusion zones), we just introduce a certain amount of crack adaptability within each element. The rationale behind the method is that the estimation of the principal directions in a triangular element is specially bad at crack initiation due to the high stress gradients in the crack tip zone where the new cracked element is usually located; after the crack grows further, the estimation of the principal stress directions usually improves substantially. Therefore we allow the crack to adapt itself to the later variations in principal stress direction *while its opening is small*.

This crack adaptation is implemented very easily by stating that while the equivalent crack opening ϖ is small, the crack direction is recomputed at each step as if the crack were freshly created. After ϖ reaches a threshold value ϖ_{th} , no further adaptation is allowed and the crack direction becomes fixed. Threshold values must be related to the softening properties of the material, and values of the order of $0.1-0.2 G_F/f_t$ are usually satisfactory.

This simple expedient has proved to be extremely effective as shown in the examples presented next, and bears some resemblance with other approaches used to avoid crack locking. For example, Tano et al. [11] used a rotating crack model to avoid locking and Jirásek and Zimmermann [7] in which a smeared rotating crack model was introduced at the beginning of cracking. In our approach the crack adaptation is introduced to circumvent the numerical deficiency in predicting accurately the principal stress directions, and has not to be taken as a material property.

4 MODE I TESTS

The model described in the preceding sections has been implemented through user subroutines in two commercial finite element programs: FEAP and ABAQUS. As a reference, the program Splitting-Lab, based on a highly accurate boundary integral approach (smeared-tip method; see Bazant & Planas [12]), was used to compute the results for the bending beam

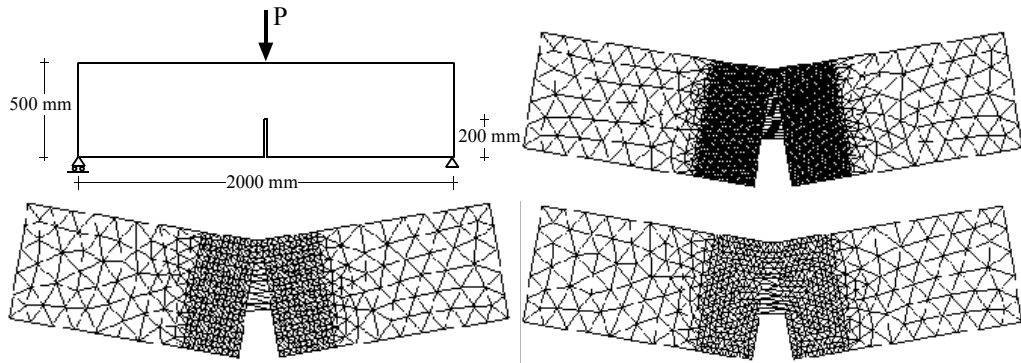


Figure 2: Three point bending test beam dimensions (top left), fine structured mesh (3664 elements, top right), coarse structured mesh (1110 elements, bottom left), and coarse unstructured mesh (1166 elements, bottom right).

The three point bending beam test defined in Figure 2 was analyzed using three finite element meshes. The material parameters were taken to be as follows: tensile strength $f_t = 2.5$ MPa, Young modulus $E = 20$ GPa, Poisson's ratio $\nu = 0.15$ fracture energy $G_F = 0.1$ N/mm. An exponential softening curve for the cohesive crack model was adopted for simplicity. The computations were run under control of the displacement at the upper midpoint.

Figure 3 shows, on the left, the load-displacement curves computed *without* crack adaption together with a reference curve computed using the smeared-tip superposition method. Obviously, the response of the finite element computations is too stiff and the computation stops prematurely because of crack locking and lack of convergence. When crack adaption is introduced (Fig. 3 right) the results drastically change: crack locking disappears and the response for all three meshes is excellent, although the coarse structured mesh strengthens the response in the tail of the curve. The coarse unstructured mesh follows the tail with surprising accuracy. There is no trace of spurious mesh sensitivity. Note also that the crack path is perfectly traced in all three meshes as shown in the deformed meshes of Figure 2.

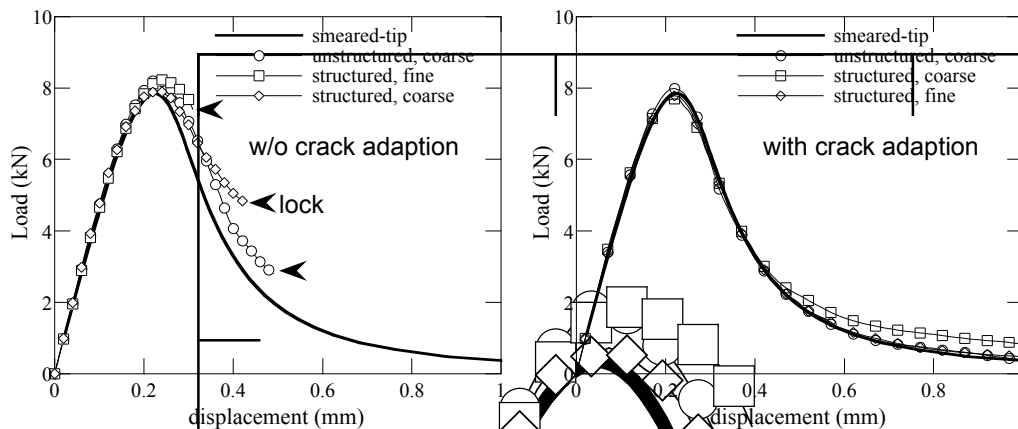


Figure 3: Numerical results for the TPB test with the three different meshes used, without crack adaption (left) and with crack adaption (right).

5 MIXED MODE TESTS

To show the ability of the proposed approach to follow cracking in other cases, several experimental results in the literature have been analyzed. As an example, we report here the analysis of the tests by Schlangen [13,14] and Shi et al. [15].

Figure 4 shows the geometry of one of the Schlangen's tests on notched beams in four-point-shear together with the deformed coarse mesh with 461 elements and the comparison of the measured and computed load versus CMOD curve. No locking occurs, the crack path of the crack is correctly captured, and the peak load and initial part of the curve are correctly predicted by the model. The prediction of the tail could be improved by selecting a softening curve with a steeper initial descent and a stronger tail.

Figure 5 shows the asymmetric double-edge-notch specimens of Shi et al. Also shown is the relatively finer mesh used for computations and the comparison of the experimental and computed load-displacement curves. Again, no locking occurs, the cracks are correctly captured. In this case, the computed response is surprisingly close to the experimental results.

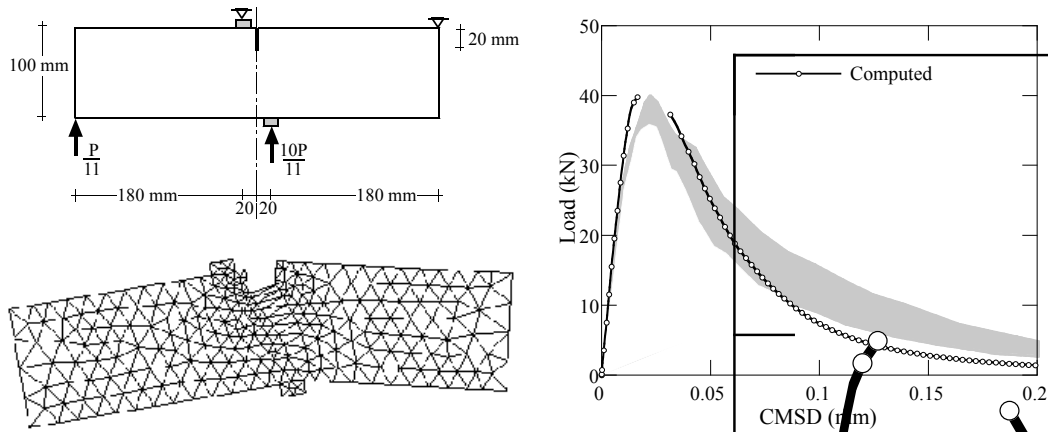


Figure 4: Schlangen's tests [13,14]. Material properties from [5]: $E = 35$ GPa, $\nu = 0.15$, $f_t = 2.8$ MPa, $G_F = 100$ N/m. Exponential softening used in computations.

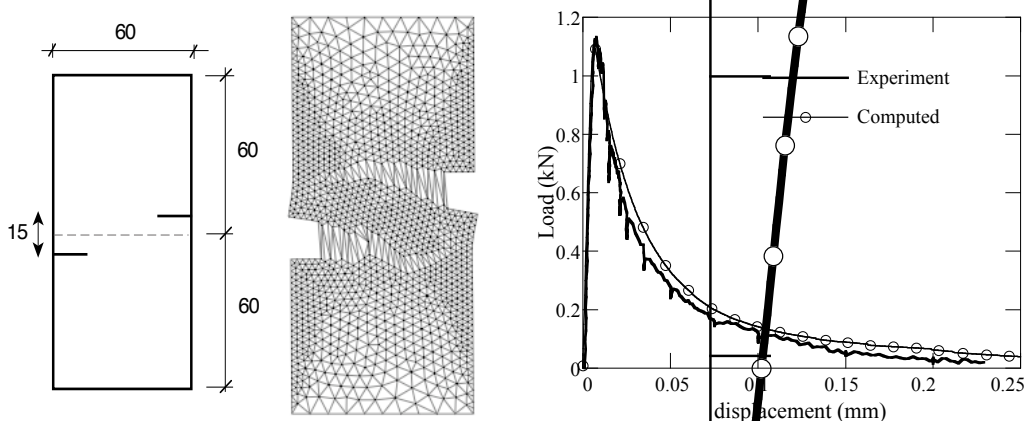


Figure 5: Tests of Shi et al. [15]. Material properties: $E = 31$ GPa, $\nu = 0.2$, $f_t = 3.0$ MPa, $G_F = 50$ N/m. Exponential softening used in computations.

6 FINAL REMARKS

The foregoing results show that a fortunate combination of simple ingredients has been found that leads to the automatic propagation of the cohesive crack without the need for tracking algorithm or exclusion zones. The stress-locking effects are solved by letting the embedded crack in the finite element to adapt itself to the stress field while the crack opening does not exceed a small threshold value. The numerical simulations show that the embedded crack approach is yet an effective and simpler alternative to other more sophisticated methods for the simulation of concrete damage and fracture.

ACKNOWLEDGMENTS. The authors gratefully acknowledge financial support from the Spanish Ministerio de Ciencia y Tecnología under grant MAT2001-3863-C03-01/02.

REFERENCES

- [1] Simo, J., Oliver, J. & Armero, F., An analysis of strong discontinuities induced by strain softening in rate-independent inelastic solids, *Computational Mechanics*, 12, 277-296, 1993.
- [2] Oliver, J., Modelling strong discontinuities in solid mechanics via strain softening constitutive equations; Part 1: fundamentals; Part 2: numerical simulations, *International Journal for Numerical Methods in Engineering*, 39, 3575-3623, 1996.
- [3] Jirásek, M., Comparative study on finite elements with embedded cracks, *Computer Methods in Applied Mechanics and Engineering*, 188, 307-330, 2000.
- [4] Wells, G.N., Discontinuous modeling of strain localization and failure, Ph D. Thesis Delft University of Technology, 2001.
- [5] Alfaiate, J., Wells, G.N. & Sluys, L.J., On the use of embedded discontinuity elements with path continuity for mode-I and mixed-mode fracture, *Engineering Fracture Mechanics*, 69, 661-686, 2002.
- [6] Feist, C., & Hofstetter, G., Mesh-insensitive strong discontinuity approach for fracture simulations of concrete, Proc. Numerical Methods in Continuum Mechanics, NMCM 2003, CD-ROM, 2003.
- [7] Jirásek, M., & Zimmermann, T., Embedded crack model Part II: Combination with smeared cracks, *International Journal for Numerical Methods in Engineering*, 50, 1291-1305, 2001.
- [8] Oliver J. , Huespe, A. E., Samaniego, E. & Chaves, E.W.V., On strategies for tracking strong discontinuities in computational failure mechanics. *Fifth World Congress on Computational Mechanics*, Vienna, Austria, 2002.
- [9] Sancho, J.M., Planas, J. & Cendón, D.A., An embedded cohesive crack model for finite element analysis of concrete fracture, *Fracture Mechanics of Concrete Structures*, Li et al (eds), Ia-FraMCoS, ISBN 0-87031-135-2, pp. 107-114, 2004.
- [10] Borja, R.I., A finite element model for strain localization analysis of strongly discontinuous fields based on standard Galerkin approximation, *Computer Methods in Applied Mechanics and Engineering*, 190, 1529-1249, 2000.
- [11] Tano, R., Klisinski, M. & Olofsson, T., Stress locking in the inner softening band method: A study of the origin and how to reduce the effects, *Computational Modelling of Concrete Structures*, De Borst, Bicanic, Mang & Meschke (eds), Balkema, Rotterdam, pp. 329-335, 1998.
- [12] Bazant, Z.P. & Planas, J., *Fracture and Size Effect of Concrete and Other Quasibrittle Materials*. CRC Press, Boca Raton, FL, USA, 1998.
- [13] Schlangen. E., Experimental and numerical analysis of fracture processes in concrete. Ph D. Thesis Delft University of Technology, 1993.
- [14] Schlangen, E. & van Mier, J.G., Mixed-mode fracture propagation: a combined numerical and experimental study, *Fracture and damage of concrete and rock*, H.P. Rossmanith (ed), E&FN SPON, London, pp. 166-175, 1993.
- [15] Shi, C., van Dam, A.G., van Mier, J.G.M. and Sluys, L.J., "Crack interaction in concrete", *Materials for Buildings and Structures EUROMAT*, Wittmann Ed., 6, 125-131, 2000.